Textile & Leather Review

ISSN 2623-6281| www.tlr-journal.com | 10.31881/TLR

Parameter Optimization of Functional Textile Materials for Building Sunshade Based on Multi-Objective Genetic Algorithm

Lei Guo

How to cite: Guo L. Parameter Optimization of Functional Textile Materials for Building Sunshade Based on Multi-Objective Genetic Algorithm. Textile & Leather Review. 2026; 9:807-827. https://doi.org/10.31881/TLR.2026.807

How to link: https://doi.org/10.31881/TLR.2026.807

Published: 31 March 2026

Parameter Optimization of Functional Textile Materials for Building Sunshade Based on Multi-Objective Genetic Algorithm

Lei Guo

Architectural Engineering Institute, Shandong Business Institute, Yantai 265199, Shandong, China
guolei_202020@163.com

Article
https://doi.org/10.31881/TLR.2026.807
Received 29 July 2025; Accepted 25 August 2025; Published 31 March 2026

ABSTRACT

Existing functional textile materials for building shading lack effective methods for parameter coordination and optimization across multiple performance objectives, making it difficult to simultaneously meet comprehensive requirements for shading, light transmission, and energy savings. To address this issue, this paper proposes a parameter optimization framework based on a multi-objective genetic algorithm (MOGA). It constructs a performance model with fabric density, coating thickness, and fiber thermal conductivity as variables, and shading efficiency, visible light transmittance, and thermal resistance as objective functions. MOGA is employed to optimize these parameters and obtain an optimal solution set that achieves coordinated multi-performance. Experimental results show that changes in coating thickness and thermal conductivity significantly affect visible light transmittance and thermal resistance, verifying the effectiveness of the multi-objective genetic algorithm for optimizing building shading materials. This has important engineering application value.

KEYWORDS

multi-objective genetic algorithm, functional textile materials, performance evaluation model, visible light transmittance, thermal resistance

INTRODUCTION

In the context of increasing demand for building energy conservation and indoor thermal environment control, shading systems play a key role in energy conservation as well as light and heat control. Functional textile materials [1,2] are widely used in building shading systems [3] due to their light weight, flexibility, ease of

processing, and adjustable performance, and have become the core medium for controlling building thermal and light performance. These materials must balance multiple properties to adapt to complex building environments [4,5]. However, functional textile materials for shading have many parameters, complex coupling relationships, and significant difficulties in performance optimization [6,7]. Currently, most studies ignore the synergy between multiple properties and lack systematic multi-objective optimization methods [8,9]. Additionally, traditional optimization methods are mostly based on empirical judgment or single-objective search [10], making it difficult to obtain design solutions with balanced overall performance when multi-objective conflicts exist, thereby limiting the maximum utilization of material performance in practical applications.

In recent years, innovations in the integration of materials and structural design have continued to demonstrate the potential of textile materials in architectural regulation [11,12]. Procaccini et al. [13] clarified the comprehensive advantages of textile membranes for sunshading by examining their characteristics and establishing a classification framework. Cui et al. [14] introduced multi-objective optimization and modeling analysis, proposed a lightweight sunshade prototype, and optimized both sunshade efficiency and structural adaptability. Denz et al. [15] developed adaptive sunshade materials by embedding shape memory alloys. Although these studies have made positive progress in structural innovation and parametric optimization [16], there is still a lack of in-depth modeling and system integration of the trade-offs and synergy mechanisms among multi-dimensional performance indicators for functional textile materials [17,18].

In research on the performance optimization of functional textile materials [19,20], MOGA has become an important tool for improving the comprehensive performance of materials [21]. Zani et al. [22] used a multi-objective genetic algorithm to optimize sunshade performance and enhance comfort and visual connectivity. Das et al. [23] constructed an SVR-genetic algorithm model to demonstrate the advantages of MOGA in multi-index coordination. Ahlawat et al. [24] combined neural networks with MOGA to optimize 3D-printed carbon fiber nylon materials. Although MOGA has performed well with various materials, there is still a lack of dedicated models and design frameworks for coordinated optimization of thermal and optical properties in sunshade textile materials [25,26].

To fill this research gap, this paper proposes a parameter optimization method for functional textile materials for building shading based on MOGA, focusing on the needs for light and heat regulation. Using fabric density,

coating thickness, and fiber thermal conductivity as variables, the objective function is constructed; the coupling relationships with shading efficiency, transmittance, and thermal resistance are clarified; the MOGA evaluation mechanism is adapted through standardization. During the optimization process, a thermal and optical performance trade-off function is constructed, and a stable Pareto frontier solution set is obtained through non-dominated sorting and crowding control. A multi-attribute decision-making method is further introduced to select representative configurations and improve the synergy of thermal comfort, energy savings, and visual performance. This method provides both theoretical and practical support for research and development of functional textile materials in the field of building energy conservation. The optimization framework introduces a parameter normalization strategy based on performance response curvature, and a dynamic weight allocation mechanism that enhances the algorithm's convergence stability under conflicting thermal and optical performance objectives. The nonlinear correlation of fabric structural parameters under the optical-thermal coupling mechanism, and their sensitivity in the medium and high value ranges, make it difficult for the standard MOGA algorithm to maintain a balanced distribution on the Pareto front without improvements. This framework effectively addresses this issue by jointly controlling convergence accuracy and solution sparsity.

CONSTRUCTION AND ALGORITHM IMPLEMENTATION OF THE MULTI-PERFORMANCE OPTIMIZATION MODEL FOR SUNSHADE FABRIC

Establishment of the Parameter System for Functional Fabrics for Building Shading

This study takes fabric density x_1, coating thickness x_2, and fiber thermal conductivity x_3 as the three core design variables of sunshade fabrics and constructs a structural parameter vector. To achieve unified scale processing, the following methods are used for normalization:

Fabric density is expressed in g/m² to ensure consistency with Figures 1–4 and related descriptions. Fabric density x_1: the value range is [$x_{1_{min}}$, $x_{1_{max}}$]. The power function is normalized, and the unit is g/m²:

$$x_1^* = \frac{x_1 - x_{1_{min}}}{x_{1_{max}} - x_{1_{min}}} \quad (1)$$

Coating thickness x_2: the value range is [$x_{2_{min}}$, $x_{2_{max}}$], using power function normalization:

$$x_2^* = \left(\frac{x_2 - x_{2_{min}}}{x_{2_{max}} - x_{2_{min}}}\right)^{\alpha} \quad (2)$$

Where, α is the mapping curvature adjustment factor. The value of α is based on nonlinear response curve fitting results for shading efficiency and transmittance at different coating thicknesses, and is set to 1.35 by least squares regression, making the normalized curve more sensitive to performance changes in the medium and high value range.

Fiber thermal conductivity x_3: the domain is $[x_{3_{min}}, x_{3_{max}}]$, using reciprocal mapping:

$$x_3^* = \frac{1}{1 + \lambda x_3} \quad (3)$$

Where,λ controls the smoothness of the mapping function. In this study, smoothness is determined by the normalized interval endpoints and the reciprocal function form, without introducing additional parameters. The three standardized variables x_1^*, x_2^*, and x_3^* constitute the structural parameter input vector, providing a consistent scale input basis for subsequent multi-objective function modeling and optimization.

Modeling and Normalization of Multiple Performance Objective Functions

Modeling Expressions for Shading Efficiency, Transmittance, and Thermal Resistance

Optimizing the performance of shade fabrics involves three key objective functions:

Shading efficiency f_1 measures the ability of fabric to block direct solar radiation and is defined as:

$$f_1 = 1 - \frac{E_t}{E_i} \quad (4)$$

Where, E_i is the incident solar radiation energy per unit area, and E_t is the radiation energy transmitted through the fabric. E_t is calculated using a modified radiation transfer model based on fabric density, coating thickness, and thermal conductivity. Fabric density affects porosity; coating thickness changes the scattering and absorption path length for light; thermal conductivity indirectly affects optical absorption characteristics through the material composite ratio. To support this mechanism, the optical model introduces complex refractive index parameters (n, k) measured from representative fiber samples, combined with an interface

scattering correction based on Fresnel reflection at fabric–coating boundaries. These parameters are integrated into regression fitting to link thermal conductivity variation with changes in reflectivity and absorption efficiency. The function is determined by the design variables x_1, x_2, x_3.

Visible light transmittance f_2 indicates the average transmittance of fabrics in the visible light band and is defined as:

$$f_2 = \frac{\int_{\lambda_1}^{\lambda_2} \tau(\lambda,\vec{x}) \cdot I(\lambda)\, d\lambda}{\int_{\lambda_1}^{\lambda_2} I(\lambda)\, d\lambda} \tag{5}$$

Where, $\tau(\lambda,\vec{x})$ is the spectral transmittance at wavelength λ, and $I(\lambda)$ is the spectral irradiance in the visible band: λ_1= 400 nm, λ_2= 760 nm. The weighting process adopts the CIE 1924 photopic visual function V(λ) rather than spectral irradiance, ensuring consistency with the standard definition of visible light transmittance. Before measurement, the spectrophotometer was calibrated using a certified reference white plate to correct baseline drift. Spectral transmittance has an exponential decay relationship with fabric density and a piecewise linear decay relationship with coating thickness. Changes in thermal conductivity alter the transmission efficiency of certain bands through the material interface structure. These relationships are obtained by regression fitting to experimental data.

Thermal resistance f_3 reflects the resistance of the fabric to heat conduction and is defined as:

$$f_3 = \frac{d_{\mathrm{eq}}}{k_{\mathrm{eq}}} \tag{6}$$

Where, d_{eq} is the equivalent thickness, and k_{eq} is the equivalent thermal conductivity, both determined by the physical parameters and structure of the fabric and coating. Equivalent thickness is determined by the sum of the fabric substrate thickness and the coating thickness. Equivalent thermal conductivity is determined by a series thermal resistance model, in which the fabric substrate and coating layers transmit heat sequentially along the thickness direction. This approach reflects the actual stacking structure of the fabric system and avoids assuming simultaneous heat transfer in parallel. Fabric density affects the density of fiber arrangement. Coating thickness and thermal conductivity jointly determine the thermal conduction path and resistance of the composite system.

The three performance functions use the structural design variables $\vec{x}=[x_1,x_2,x_3]$ as independent variables and constitute the objective vector of the multi-objective optimization problem:

$$\vec{F}(\vec{x})=[f_1(\vec{x}),f_2(\vec{x}),f_3(\vec{x})] \quad (7)$$

The above functions combine physical mechanism modeling and experimental fitting to ensure each performance objective in the optimization responds appropriately to variable changes.

Standardization and trade-off methods for multi-objective functions

To unify the scale of the objective function and avoid interference from differences in physical dimensions during fitness evaluation, the three objective functions f_1, f_2, and f_3—need to be standardized.

Standardization: Assuming that the minimum and maximum values of the objective function f_i are $f_i^{\min}$ and $f_i^{\max}$, respectively, the standardized form is as follows:

$$f_i^{\text{norm}}=\frac{f_i-f_i^{\min}}{f_i^{\max}-f_i^{\min}} \quad (8a)$$

For visible light transmittance f_2, which needs to be minimized, the inverse transformation is used to ensure directional consistency:

$$f_2^{\text{norm}}=1-\frac{f_2-f_2^{\min}}{f_2^{\max}-f_2^{\min}} \quad (8b)$$

Performance trade-off processing: The weighted comprehensive performance function is introduced as follows:

$$F_{\text{comp}}=\sum_{i=1}^{3} w_i \cdot f_i^{\text{norm}} \quad (9)$$

Where, w_i is the weight coefficient of the i-th objective, satisfying $\sum w_i = 1$.

A dynamic weight strategy σ_i is used to calculate the weight according to the standard deviation of each objective function in the current population:

$$w_i = \frac{\sigma_j}{\sum_{j=1}^{3} \sigma_j} \tag{10}$$

The crowding distance calculation is used to measure the sparsity of non-dominated solutions in the objective space. Suppose that, for the objective function, the adjacent values of the current individual before and after are f_i^+ and f_i^-, respectively. The crowding degree in this dimension is:

$$CD_i = \frac{f_i^+ - f_i^-}{f_i^{max} - f_i^{min}} \tag{11}$$

The sum of the three-dimensional crowding degrees is used for individual priority sorting, assisting in diversity preservation and elite selection.

Multi-objective Genetic Algorithm Optimization Process Design

Real Number Coding and Initial Population Construction

In the initialization stage, to achieve accurate representation of continuous design variables, real number coding is used to numerically represent the fabric density (x_1), coating thickness (x_2), and fiber thermal conductivity (x_3).

The population size is set to P, and each individual is a parameter vector $x = (x_1, x_2, x_3)$ of length 3, where the domains of the variables are $[x_{1_{min}}, x_{1_{max}}]$, $[x_{2_{min}}, x_{2_{max}}]$, $[x_{3_{min}}, x_{3_{max}}]$. The initial population is generated by pseudo-random uniform sampling, and the expression is as follows:

$$x_i = x_{i_{min}} + r_i \cdot (x_{i_{max}} - x_{i_{min}}),\ r_i \in (0,1) \tag{12}$$

The above method ensures the uniform distribution of the initial solution set in the parameter space. The continuous individuals generated by real number coding do not require discretization or bit weight conversion and can be directly used for fitness evaluation, making them suitable for subsequent simulated binary crossover and normal mutation operations.

The multi-objective genetic algorithm used in this study employs a population size of 200, 300 evolutionary generations, a simulated binary crossover probability of 0.9, a mutation probability of 0.05, a distribution exponent of 20, and a standard deviation adjustment factor initialized at 0.1 and linearly decreased to 0.01

over the course of the iterations. These parameters were determined after comparing convergence speed and distribution uniformity across multiple pilot experiments.

Non-dominated Sorting, Fitness Evaluation, and Evolutionary Mechanism

Non-dominated sorting is used to determine the quality of individuals in multi-objective optimization and to construct a Pareto hierarchy structure. Assume the current population size is N, and the objective function vector of the i-th individual is $F_i = (f_1, f_2, f_3)$, corresponding to the maximization objectives of shading efficiency and thermal resistance, and the minimization objective of transmittance (equivalently, maximization of shading efficiency defined as 1 − transmittance). If an individual A satisfies: $f_j(A) \geq f_j(B)$, and at least one objective is strictly greater, it is called A dominant B, denoted as $A \succ B$. All individuals are divided into multiple non-dominated levels according to the dominance relationship $F_1, F_2, \ldots$.

To maintain the diversity of solutions, crowding distance is introduced as an evaluation indicator. Let the maximum and minimum values of the j-th in the current level is f^j_{max} and f^j_{min}, respectively. For the i-th individual, its crowding distance under this objective is calculated as:

$$d_j(i) = (f_j(i+1) - f_j(i-1)) / (f^j_{max} - f^j_{min}) \quad (13)$$

The total crowding distance for the three objectives is:

$$CD(i) = \sum_j d_j(i) \quad (14)$$

The larger the crowding distance, the more sparsely located the individual is in the target space and should be retained first.

The evolution process adopts a fast tournament selection strategy, selecting individuals according to the priority of non-dominated level and the order of crowding distance. The crossover operation uses the simulated binary crossover method. Let the two parent individuals be $x_1$and x_2; the j-th dimension variable generates two offspring expressions as:

$$c_{1j} = 0.5[(1+\beta)x_{1j} + (1-\beta)x_{2j}] \quad (15)$$

$$c_{2j} = 0.5[(1-\beta)x_{1j} + (1+\beta)x_{2j}] \quad (16)$$

$$\beta=(2r)\wedge\{1/(\eta+1)\},r\in(0,1) \quad (17)$$

Where, η is the distribution exponent, which controls the interpolation density of the solution.

The mutation operation adopts the Gaussian perturbation model. Assume that the mutation of the i-th dimension variable of the j-th individual is:

$$x_j^{'}=x_j+\sigma_j\cdot N(0,1) \quad (18)$$

Where, $\sigma_j$is the standard deviation adjustment factor, which is gradually reduced with evolutionary generations to enhance local convergence.

Each generation iteration merges the parent and offspring populations, re-performs non-dominated sorting and crowding evaluation, and selects the first N individuals to form a new generation population.

This process maintains the co-evolution of optimal solutions among multiple objective functions, ensuring that fabric parameter configuration achieves global optimization of a reasonable structure under the goals of sun shading, light transmittance, and heat insulation.

Elite Retention Strategy and Pareto Frontier Extraction

In the optimization process of the multi-objective genetic algorithm, the elite retention mechanism is used to ensure the continuous inheritance of high-quality solutions and the stable evolution of non-dominated solutions. In each generation, the parent population $P_t$and the child population Q_t are merged into an intermediate population R_t, which is then divided into multiple level sets after non-dominated sorting F_1, F_2, F_3. When updating the population, F_1individuals of each level are added to the next generation population in sequence from the beginning P_{t+1}until the set size N is approached. When the total number of individuals $F_k$of a certain level exceeds the upper limit, the level is sorted from large to small according to crowding distance, and the top-ranked individuals are retained to fill the vacancies. The crowding distance is used as a measure of the boundary representativeness of individuals in the target space, and solutions located in sparse areas or boundary positions are preferentially retained to maintain the diversity and structural integrity of the population distribution.

After each generation of iteration, the solutions $F_1$with level are extracted to form the contemporary Pareto

frontier solution set, which is then merged with the frontier solution set of the historical generation, and the global optimal solution set is formed through re-sorting and redundant elimination.

Solution Set Screening and Optimal Parameter Identification Method

Multi-Attribute Decision-Making Method for Representative Solution Selection

To select a representative structural combination with balanced performance from the non-dominated solution set, this paper adopts the approximate ideal solution sorting method to perform multi-attribute decision analysis. First, the objective function matrix of the candidate solutions is vector-normalized to obtain a standardized matrix R, whose elements r_{ij} are calculated as follows:

$$r_{ij}=r_{ij}\div\sqrt{(r_{1j}^2+r_{2j}^2+\cdots+r_{mj}^2)} \tag{19}$$

Where, i represents the i-th solution; j represents the j-th objective function; m is the total number of candidate solutions.

The weight vector is determined according to the importance of each target w_j, objective, satisfying $\sum w_j = 1$. The elements of the weight matrix V are calculated as follows:

$$v_{ij}=w_j\times r_{ij} \tag{20}$$

Negative a^- ideal solutions are constructed using the maximum and minimum values of each column a^+ in the objective matrix. The distances from solution i to the positive and negative ideal solutions are calculated as:

$$d_i^+=\sqrt{[(v_{1i}-a_1^*)^2+(v_{12}-a_2^*)^2+(v_{13}-a_3^*)^2]} \tag{21}$$

$$d_i^*=\sqrt{(v_{1i}-a_{1i})^2+(v_{12}-a_{2i})^2+(v_{13}-a_{3i})^2} \tag{22}$$

The proximity index is then computed based on this C_i: these distances:

$$C_i=d_i^-\div(d_i^+ +d_i^-) \tag{23}$$

Finally C_i, the solution with the largest proximity index is selected, and its structural parameter vector is regarded as the representative solution: $x_{rep}=X(_{imax})$.

After screening representative combinations with balanced performance, it is necessary to further evaluate the feasibility of these combinations in engineering applications to ensure that the optimization results can be smoothly translated from the theoretical stage to actual production and use.

Logic for Determining the Engineering Suitability of the Optimal Parameter Combination

To ensure that the representative solution is not only optimal in mathematical terms but also possesses engineering practicality, a joint assessment is required from two perspectives: performance index satisfaction and structural parameter processability. The three structural parameters constituting the representative solution are fabric density, coating thickness, and fiber thermal conductivity, which correspond to shading efficiency, visible light transmittance, and thermal resistance performance, respectively.

These thresholds are derived from building shading design guidelines and ISO 15099 standard recommendations, which specify reference values for acceptable solar shading efficiency, visible light transmittance, and thermal resistance in façade applications. In terms of performance, the minimum acceptable thresholds are shading efficiency not less than 0.85, transmittance not higher than 0.25, and thermal resistance not less than 0.030 $m^2 \cdot K/W$. If all three performance criteria are met, the solution is considered effective; if some values are slightly below the standards, the solution is evaluated based on the degree of deviation and the corresponding target weight to determine its potential for adjustment, and it is classified as a suboptimal solution.

The adaptability of structural parameters is determined by comparing whether they fall within the feasible range of current weaving and coating processes. Fabric density must balance yarn distribution and the integrity of light holes; coating thickness should be controlled within the limits of hot melt or heat-setting treatments; and the thermal conductivity coefficient must be within the range typical for common fiber raw materials (such as polyester and composite fibers). If all three variables meet the actual process requirements and do not cause structural instability or failure in the thermal conduction model, the solution is deemed structurally adaptable.

In summary, if both performance and structural criteria are satisfied, the solution can proceed directly to sample preparation and engineering verification. If performance is suboptimal but the structure is suitable,

it is included in the fine-tuning optimization sequence. This two-level discrimination system ensures that the optimized solution not only offers theoretical performance advantages but also practical feasibility for manufacturing and application, achieving effective integration from parameter design to engineering implementation.

OPTIMIZATION PERFORMANCE ANALYSIS OF SUNSHADE FUNCTIONAL FABRICS

Experimental Setup and Measurement Method

To verify the effectiveness and reliability of the established multi-objective optimization model, a comprehensive test platform operating under constant temperature and humidity conditions was built. The laboratory temperature was maintained at 25 ± 1 °C, and relative humidity was kept at 50 ± 5%. No external light sources or air flow interfered during testing. The specimens comprised three levels of fabric density, three coating thicknesses, and three fiber thermal conductivities, resulting in a total of 27 combinations. Each fabric combination used a plain weave structure and underwent standardized heat-setting treatment to eliminate dimensional stress differences caused by weaving and coating processes. The coating was applied using a hot melt process with thicknesses ranging from 100 μm to 500 μm. Thermal conductivity was controlled by selecting different fiber types and composite ratios.

Shading efficiency was measured using a DHI-3000 solar simulator with a light intensity of 1000 W/m² and a spectral range of 300–2500 nm. Incident light was directed perpendicularly to the center of each specimen. Transmitted light energy was measured with an integrating sphere and spectral analysis system, and shading efficiency was calculated based on incident energy. Visible light transmittance was measured using a UV-3600 spectrophotometer covering the 400–760 nm wavelength range. During testing, specimens were clamped flat in the optical path, and the spectral transmittance curve was scanned point by point. The average transmittance was calculated using a normalized weighted method. Thermal resistance was measured with a YG(B)606E fabric thermal resistance tester under a test pressure of 49 Pa and a measurement area of 100 cm². The temperature differential was maintained at 10 ± 0.2 °C. The instrument automatically recorded the steady-state heat flow and calculated the corresponding thermal resistance value.

All tests were conducted under identical environmental conditions, with each parameter combination repeated three times and the average value taken to minimize random errors. The preprocessed test data were

then compared with the model calculation results to verify the accuracy of the performance response curves and optimization outcomes. The surrogate model was constructed using a support vector regression approach trained on the 27 experimental points. Five-fold cross-validation was performed to assess prediction stability, and the extrapolation range was restricted to within the convex hull of the sampled data to reduce overfitting risk.

Optimization effect of shading efficiency and structural influence mechanism

To analyze the mechanism by which fabric structural parameters influence sunshade performance, fabric density is selected as the primary variable. Various parameter combinations and algorithmic strategies are employed to compare performance response trends, as illustrated in Figure 1.

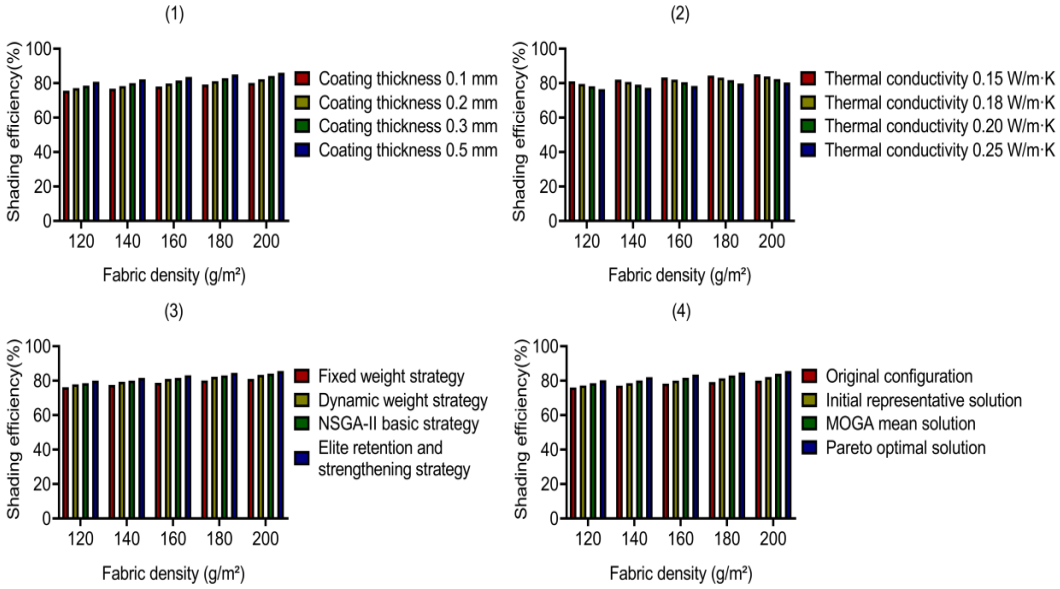

Figure 1. Trend of shading efficiency for building shading functional fabrics under multiple configuration parameters and optimization strategies. Figure 1(1): Changes in shading efficiency at different coating thicknesses; Figure 1(2): Changes in shading efficiency under varying thermal conductivity; Figure 1(3): Changes in shading efficiency under different optimization strategies; Figure 1(4): Changes in shading efficiency of different schemes along the optimized path

Figure 1 demonstrates that increasing the coating thickness from 100 μm to 500 μm raises the shading efficiency from 80.1% to 86%, indicating that greater thickness enhances the fabric's ability to block radiation.

This improvement is attributed to the extended scattering path and enlarged absorption cross-section resulting from increased coating thickness, which significantly reduces direct transmittance in the visible and near-infrared regions. Additionally, increased thickness enhances the fabric's reflection of long-wave radiation, thereby reducing the rate of surface temperature rise. In contrast, higher thermal conductivity allows heat to be conducted more rapidly along the fiber axis, which weakens the radiation-blocking effect and decreases interfacial reflectivity in the short-wavelength range, ultimately lowering shading efficiency. Specifically, when thermal conductivity increases from 0.15 W/m·K to 0.25 W/m·K, shading efficiency drops from 85.1% to 80.4%. These variation trends are analyzed under a medium fabric density of 200 g/m², which serves as a baseline for consistent comparison across different coating thickness and thermal conductivity conditions.

Improvement in the Ability to Control Visible Light Transmittance

To investigate the regulation mechanism of visible light transmittance, quantitative optical response data for each parameter were obtained through testing in the 400–800 nm wavelength band. This provides support for optimizing fabric functionality in sun shading, balanced light transmittance, and high transmittance applications, as depicted in Figure 2.

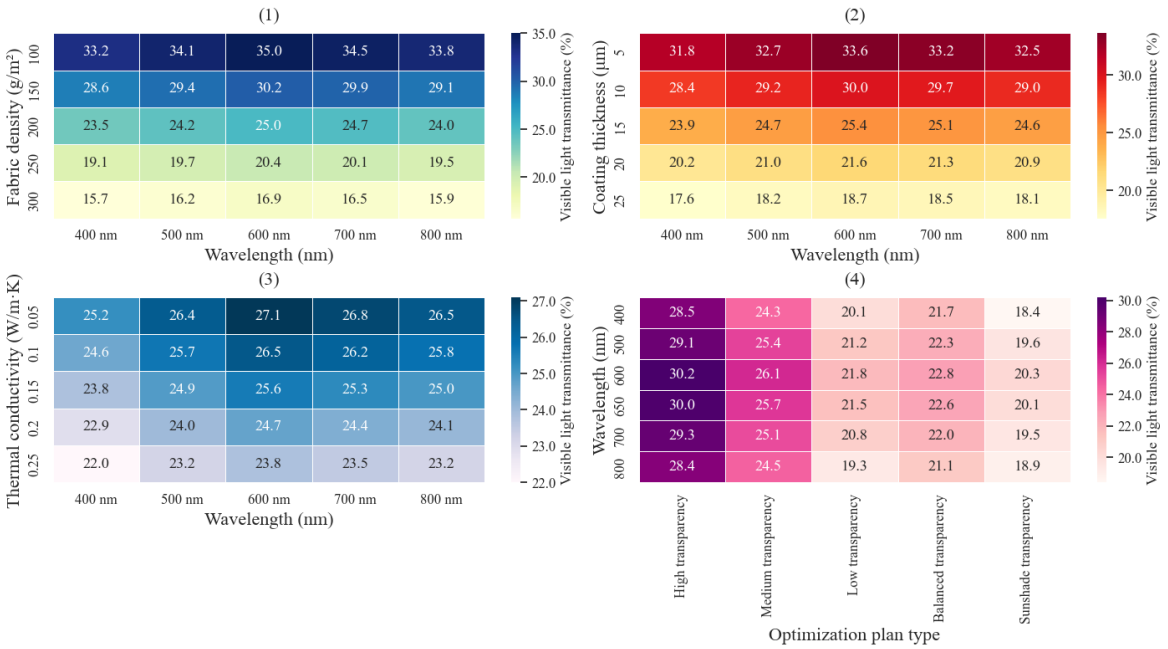

Figure 2. Comparative analysis of wavelength characteristics of visible light transmittance for fabric structural parameters and multi-objective optimization solutions. Figure 2(1): Changes in visible light transmittance at varying fabric densities and wavelengths; Figure 2(2): Changes in visible light transmittance at different coating thicknesses and wavelengths; Figure 2(3): Changes in

visible light transmittance at varying thermal conductivities and wavelengths; Figure 2(4): Changes in visible light transmittance under different solution combinations and wavelengths

Figure 2 reveals that fabric density and coating thickness are significantly negatively correlated with visible light transmittance. When density increases from 100 to 300 g/m², transmittance at the 500 nm band decreases by 17.9%. Furthermore, each 5 μm increment in coating thickness leads to an average transmittance reduction of 3.55% at 400 nm and 3.68% at 700 nm. The five optimized solutions exhibit marked differences across wavelength bands: the high-transmittance solution achieves 28.5%–29.1% transmittance in the 400–500 nm region, while the shading solution reaches as low as 18.9% transmittance in the 700–800 nm region.

Parameter Response Characteristics of Thermal Resistance Enhancement

In the assessment of the thermal performance of building sunshade fabrics, the response characteristics of thermal resistance are evaluated with respect to four variables: coating thickness, fabric density, thermal conductivity, and optimization strategy. Four typical treatment combinations are selected: C1 (cotton-plain-UV-resistant), C2 (polyester-twill-hydrophobic), C3 (linen-satin-hydrophilic), and C4 (nylon-plain-UV-resistant). Figure 3 presents the thermal resistance response results for various factor changes.

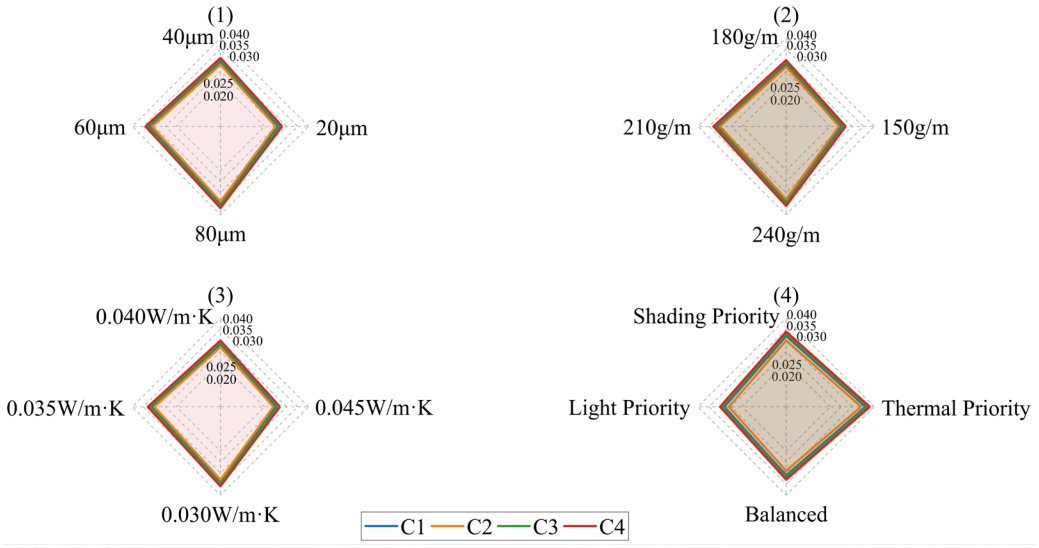

Figure 3. Radar chart of thermal resistance response characteristics for building sunshade fabrics. Figure 3(1): Thermal resistance response at different coating thicknesses; Figure 3(2): Thermal resistance response at varying fabric densities; Figure 3(3): Thermal

resistance response at different thermal conductivities; Figure 3(4): Thermal resistance response for different treatment combinations

Figure 3 indicates that thermal resistance increases with both coating thickness and fabric density. For example, in C1, thermal resistance rises from 0.026 to 0.035 m²·K/W when the coating thickness increases from 20 to 80 μm, while C4 reaches 0.037 m²·K/W under the same conditions, reflecting the superior thermal insulation of synthetic fibers. C3, featuring a dense satin weave, exhibits an increase in thermal resistance to 0.035 m²·K/W with increased density. Moreover, reducing thermal conductivity enhances thermal resistance: in C2, lowering thermal conductivity from 0.045 to 0.030 W/m·K raises the thermal resistance to 0.033 m²·K/W.

Coupling Effects of Fabric Structural Parameters on Multiple Performance Indicators

To comprehensively assess the influence of fabric structure and material parameters on multiple performance indicators, Figure 4 presents the effects of various parameters and compares typical combination performances. In Figure 4(4), G1–G5 represent the following configurations: medium-density, medium-thickness, medium-conductivity; high-density, medium-thickness, medium-conductivity; high-density, high-thickness, low-conductivity; medium-density, medium-thickness, high-conductivity; and extremely high-density, extremely high-thickness, extremely low-conductivity, respectively.

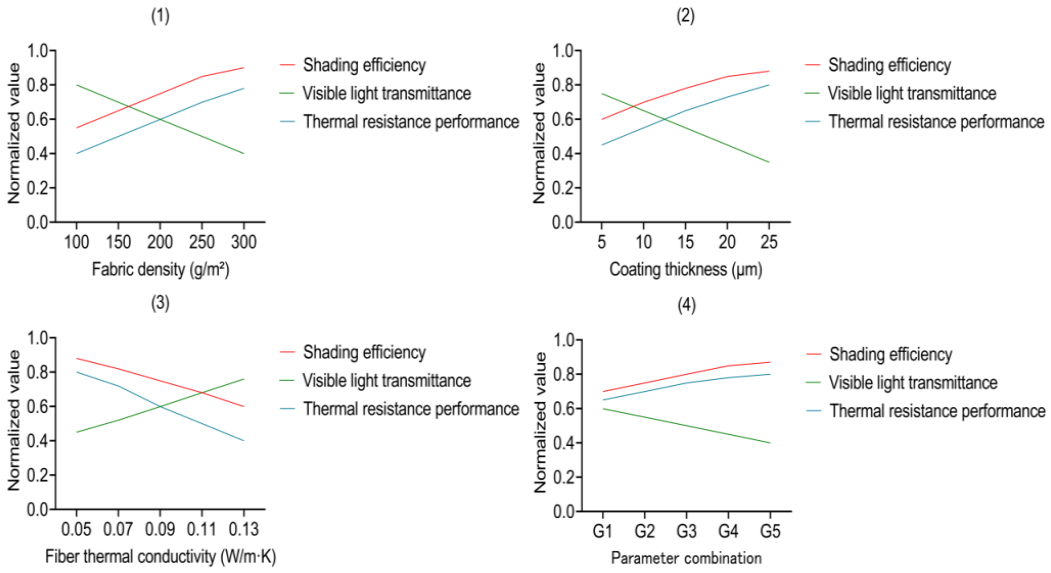

Figure 4. Effects of fabric structure and material parameters on multiple performance indicators and analysis of optimized combination performance. Figure 4(1): Effect of fabric density on multiple performance indicators; Figure 4(2): Effect of coating thickness on multiple performance indicators; Figure 4(3): Effect of thermal conductivity on multiple performance indicators; Figure 4(4): Impact of typical optimization parameter combinations on multiple performance indicators

Figure 4 indicates that increasing fabric density substantially enhances shading efficiency (from 0.55 to 0.90) and thermal resistance (from 0.40 to 0.78), while reducing transmittance (from 0.80 to 0.40). Increasing the coating thickness from 5 μm to 25 μm elevates shading efficiency to 0.88, decreases transmittance, and increases thermal resistance, underscoring its positive effect on infrared blocking. Conversely, higher thermal conductivity has the opposite effect on these performance metrics.

Engineering Suitability and Performance Comparison Evaluation of Optimized Fabric Configurations

To optimize building shading systems, a four-dimensional evaluation framework encompassing performance matching, process adaptation, stability, adjustability, and comprehensive proximity is established. Four representative solutions are selected: S1 (balanced optimal), S2 (shading dominated), S3 (lighting dominated), and S4 (insulation dominated). Figure 5 summarizes the relevant data.

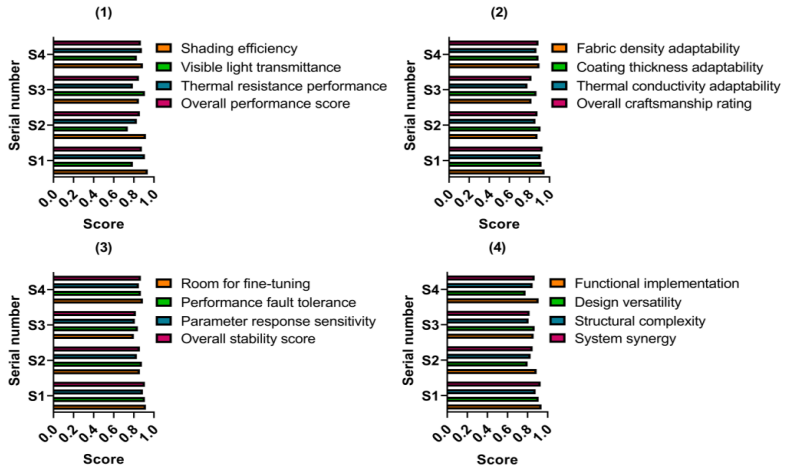

Figure 5. Comprehensive evaluation table of multi-objective shading system performance and adaptability. Figure 5(1): Performance matching evaluation; Figure 5(2): Process suitability evaluation; Figure 5(3): Evaluation of stability and adjustability; Figure 5(4): Comprehensive proximity evaluation

Figure 5 shows that S1 performs well across all dimensions, with a comprehensive performance score of 0.88,

process score of 0.93, and stability of 0.91, reflecting a high degree of balance among shading, light transmission, and thermal resistance. S2 achieves the highest shading efficiency (0.92), but its transmittance and thermal resistance scores are lower, resulting in limited versatility. S3 excels in transmittance (0.91), though its thermal resistance and process adaptability are slightly lower, prioritizing lighting applications. S4 demonstrates higher thermal resistance (0.88) and moderate stability (0.87).

CONCLUSIONS

This study introduces a multi-objective genetic algorithm (MOGA)-based optimization framework for architectural weft functional textile materials, focusing on the simultaneous optimization of key parameters such as fabric density, coating thickness, and fiber thermal conductivity. Experimental results indicate that increasing the coating thickness from 0.1 mm to 0.5 mm boosts shading efficiency from 80.1% to 86%, while raising thermal conductivity from 0.15 W/m·K to 0.25 W/m·K decreases shading efficiency by approximately 4.7%. The research verifies the coupling relationships between parameters and the balance among multiple performance metrics. However, the model is constructed under steady-state laboratory conditions and does not account for dynamic climate variations, long-term aging, or variable loading scenarios. The optimization scope is limited to the specific fabric–coating system used in these experiments. To improve physical accuracy, the thermal resistance calculation was revised to a series model, reflecting the real stacking structure of fabric and coating layers. Future research should expand the framework to include a broader range of textile structures and composite material systems, integrate dynamic environmental simulations and long-term durability assessments, and apply parallel or multi-scale optimization strategies to address large and complex parameter spaces. Such advancements would support the development of adaptive façade systems and intelligent thermal–optical regulation solutions, thereby extending the practical impact of this work to sustainable building applications and contributing to next-generation energy-efficient architectural design.

Author Contributions

All work in this study was independently completed by Lei GUO.

Conflicts of Interest

The author declares no conflict of interest.

Funding

This research received no external funding.

Acknowledgements

Not applicable.

REFERENCES

[1] Fu J, Liu T, Binte Touhid SS, Fu F, Liu X. Functional Textile Materials for Blocking COVID-19 Transmission. ACS Nano. 2023; 17(3):1739-1763. doi: 10.1021/acsnano.2c08894

[2] Fernandes M, Padrão J, Ribeiro AI, Fernandes RDV, Melro L, Nicolau T, et al. Polysaccharides and Metal Nanoparticles for Functional Textiles: A Review. Nanomaterials. 2022; 12(6):1006. doi: 10.3390/nano12061006

[3] Singh S. ArchiTextile: A Review on Application of Textiles in Architecture. Journal of Textile & Apparel Technology & Management (JTATM). 2021; 12(1). Available from: https://openurl.ebsco.com/EPDB%3Agcd%3A3%3A30101939/detailv2?sid=ebsco%3Aplink%3Ascholar&id=ebsco%3Agcd%3A149828215&crl=c&link_origin=scholar.google.com

[4] Zhang Z, Mao H, Kong Y, Niu P, Zheng J, Liu P, et al. Re-Designing Cellulosic Core–Shell Composite Fibers for Advanced Photothermal and Thermal-Regulating Performance. Small. 2024; 20(14):2305924. doi: 10.1002/smll.202305924

[5] Li M, Yan Z, Fan D. Flexible Radiative Cooling Textiles Based on Composite Nanoporous Fibers for Personal Thermal Management. ACS Applied Materials & Interfaces. 2023; 15(14):17848-17857. doi: 10.1021/acsami.3c00252

[6] He Z, Tran KP, Thomassey S, Zeng X, Xu J, Yi C. Multi-objective optimization of the textile manufacturing process using deep-Q-network based multi-agent reinforcement learning. Journal of Manufacturing Systems. 2022; 62: 939-949. doi: 10.1016/j.jmsy.2021.03.017

[7] Pakdel E, Wang X. Thermoregulating textiles and fibrous materials for passive radiative cooling functionality. Materials & Design. 2023; 231:112006. doi: 10.1016/j.matdes.2023.112006

[8] Shi B, Lookman T, Xue D. Multi-objective optimization and its application in materials science. Materials Genome Engineering Advances. 2023; 1(2):e14. doi: 10.1002/mgea.14

[9] Pătrăușanu A, Florea A, Neghină M, Dicoiu A, Chiș R. A Systematic Review of Multi-Objective Evolutionary Algorithms Optimization Frameworks. Processes. 2024; 12(5):869. doi: 10.3390/pr12050869

[10] Schwarz I, Rogale D, Kovačević S, Firšt Rogale S. A Multifunctional Approach to Optimizing Woven Fabrics for Thermal Protective Clothing. Fibers. 2024; 12(4):35. doi: 10.3390/fib12040035

[11] Zhang Y, Xia X, Ma K, Xia G, Wu M, Cheung YH, et al. Functional Textiles with Smart Properties: Their Fabrications and Sustainable Applications. Advanced Functional Materials. 2023; 33(33):2301607. doi: 10.1002/adfm.202301607

[12] Júnior HLO, Neves RM, Monticeli FM, Dall Agnol L. Smart Fabric Textiles: Recent Advances and Challenges. Textiles. 2022; 2(4):582-605. doi: 10.3390/textiles2040034

[13] Procaccini G, Prieto A, Knaack U, Monticelli C, Konstantinou T. Textile Membrane for Façade Retrofitting: Exploring Fabric Potentialities for the Development of Innovative Strategies. Buildings. 2024; 14(1):86. doi: 10.3390/buildings14010086

[14] Cui Z, Zhang S, Viscuso S, Zanelli A. Weaving Octopus: An Assembly–Disassembly-Adaptable Customized Textile Hybrid Prototype. Buildings. 2023; 13(10):2413. doi: 10.3390/buildings13102413

[15] Denz PR, Sauer C, Waldhör EF, Schneider M, Vongsingha P. Smart Textile Sun-Shading: Development of Functional ADAPTEX Prototypes. Journal of Facade Design and Engineering. 2021; 9(1):101-116. doi: 10.7480/jfde.2021.1.5539

[16] Deng W, Ke W, Deng Z, Wang X. Virtual design of woven fabrics based on parametric modeling and physically based rendering. Computer-Aided Design. 2024; 173:103717. doi: 10.1016/j.cad.2024.103717

[17] Tian Y, Ding R, Yoon SS, Zhang S, Yu J, Ding B. Recent Advances in Next-Generation Textiles. Advanced Materials. 2025; 37(8):2417022. doi: 10.1002/adma.202417022

[18] Yuan H, Liu R, Cheng S, Li W, Ma M, Huang K, et al. Scalable Fabrication of Dual-Function Fabric for Zero-Energy Thermal Environmental Management through Multiband, Synergistic, and Asymmetric Optical Modulations. Advanced Materials. 2023; 35(18):2209897. doi: 10.1002/adma.202209897

[19] Fang J, Meng C, Gao W, Zhang G, Xu Z, Min J. Agricultural waste Ipomoea batatas leaves for low-temperature dyeing and functional finishing of polyester fabrics. Industrial Crops and Products. 2024; 209:118031. doi: 10.1016/j.indcrop.2024.118031

[20] Shi S, Si Y, Han Y, Wu T, Iqbal MI, Fei B, et al. Recent Progress in Protective Membranes Fabricated via Electrospinning: Advanced Materials, Biomimetic Structures, and Functional Applications. Advanced Materials. 2022; 34(17):2107938. doi: 10.1002/adma.202107938

[21] Boukouvalas DT, Rosa JM, Belan PA, Tambourgi EB, Santana JCC, de Araújo SA. Optimization of cotton dyeing with reactive dyestuff using multiobjective evolutionary algorithms. Chemometrics and Intelligent Laboratory Systems. 2021; 219:104441. doi: 10.1016/j.chemolab.2021.104441

[22] Zani A, Speroni A, Mainini AG, Zinzi M, Caldas L, Poli T. Customized shading solutions for complex building façades: The potential of an innovative cement-textile composite material through a performance-based generative design. Construction Innovation: Information Process Management. 2024; 24(1):256-279. doi: 10.1108/CI-01-2023-0014

[23] Das S, Ghosh A. Multi-objective optimization of raw silk parameters using a combined support vector regression-genetic algorithm-desirability function approach. The Journal of The Textile Institute. 2024; 115(3):433-441. doi: 10.1080/00405000.2023.2201066

[24] Ahlawat A, Phogat A, Punia U, Chhikara A, Dhingra AK, Garg RK, et al. Innovative Optimization of Mechanical Performance in Carbon Fiber-Reinforced Nylon Composite Using Artificial Neural Networks and Multi-Objective Genetic Algorithms. Journal of Materials Engineering and Performance. 2025; 1-14. doi: 10.1007/s11665-025-10973-5

[25] Wang Y, Wu G, Zou S, Li D, Cai G. Large-scalable fabrication of zirconium carbide-based core-sheath yarn for wearable applications. Materials Today Communications. 2023; 37:106902. doi: 10.1016/j.mtcomm.2023.106902

[26] Du H, Ge C, Xu D, Qian Y, Chen Z, Gao C, et al. Multifunctional woven fabric for integrated solar-driven water generation and personal thermal management. Cellulose. 2023; 30(14):9207-9220. doi: 10.1007/s10570-023-05439-7